VIP POMs and Proton Conduction Very Important Paper

International Edition: DOI: 10.1002/anie.201803649
German Edition: DOI: 10.1002/ange.201803649

Aggregation of Giant Cerium–Bismuth Tungstate Clusters into a 3D Porous Framework with High Proton Conductivity

Jian-Cai Liu, Qing Han, Li-Juan Chen, Jun-Wei Zhao, Carsten Streb,* and Yu-Fei Song**

Dedicated to Professor Michael Thor Pope on occasion of his 85th birthday

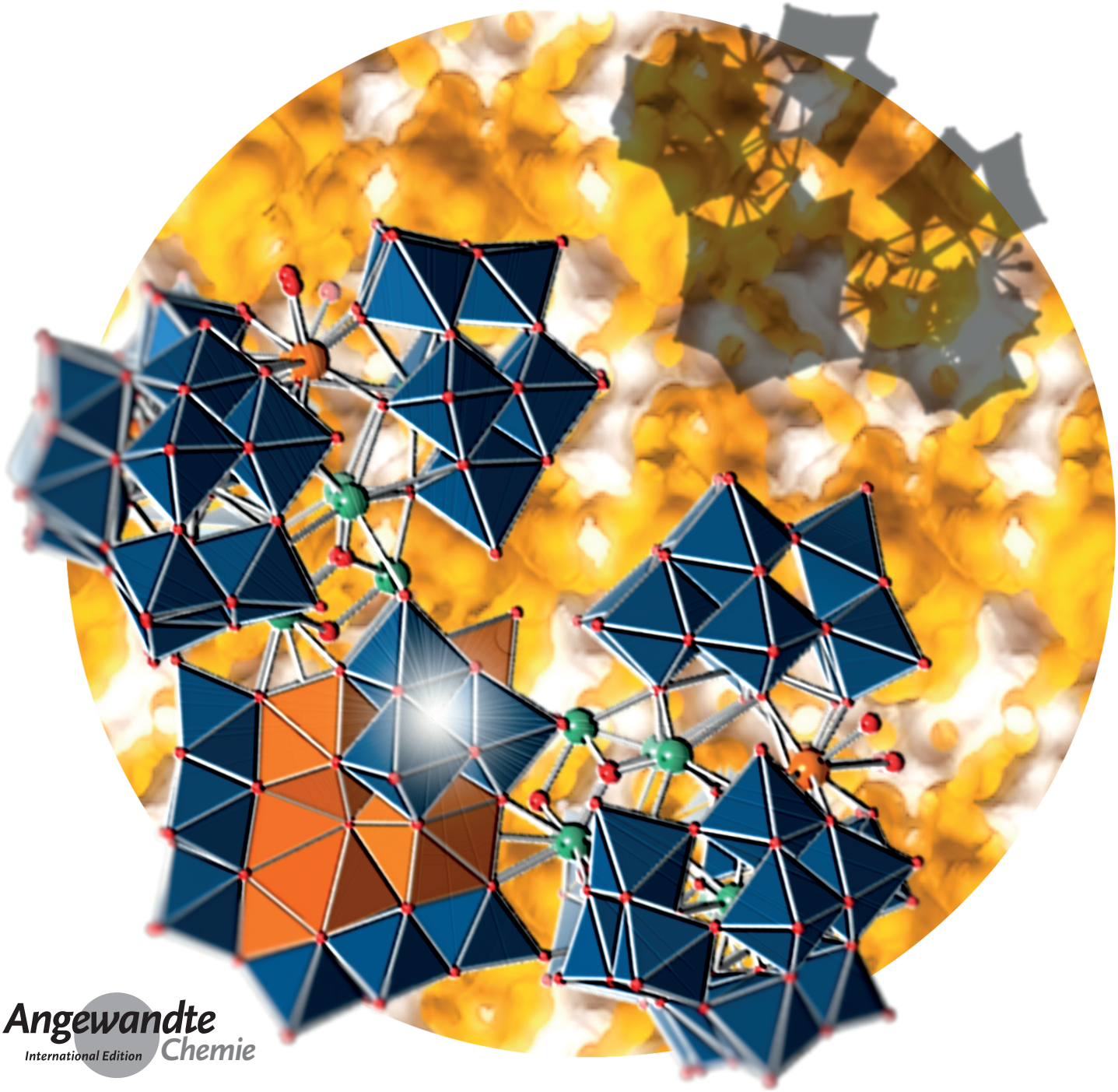

Abstract: *The exploration of high nuclearity molecular metal oxide clusters and their reactivity is a challenge for chemistry and materials science. Herein, we report an unprecedented giant molecular cerium–bismuth tungstate superstructure formed by self-assembly from simple metal oxide precursors in aqueous solution. The compound,* $\{[W_{14}Ce^{IV}_{6}O_{61}]([W_3Bi_6Ce^{III}_3(H_2O)_3O_{14}][B\text{-}\alpha\text{-}BiW_9O_{33}]_3)_2\}^{34-}$ *was identified by single-crystal X-ray diffraction and features 104 metal centers, a relative molar mass of ca. 24000 and is ca.* $3.0\times2.0\times1.7\ nm^3$ *in size. The cluster anion is assembled around a central* $\{Ce_6\}$ *octahedron which is stabilized by several molecular metal oxide shells. Six trilacunary Keggin anions (*$[B\text{-}\alpha\text{-}BiW_9O_{33}]^{9-}$*) cap the superstructure and limit its growth. In the crystal lattice, water-filled channels with diameters of ca. 0.5 nm are observed, and electrochemical impedance spectroscopy shows pronounced proton conductivity even at low temperature.*

The aggregation of molecular metal oxides into solid-state architectures offers groundbreaking opportunities for application-driven bottom-up materials design.[1–3] Molecular metal oxides, so-called polyoxometalates (POMs), are structurally well-defined metal-oxo cluster anions with far-ranging applications in catalysis, medicine, magnetism, electro-optics, conductivity and materials science.[4–6] POM anions can aggregate into larger superstructures by linkage of individual POMs using cationic metal species.[7] This reactivity is particularly well-established in polyoxotungstate chemistry, where tungstate clusters featuring one or several metal cation binding sites (so-called lacunary POMs)[8] have been bridged into giant cluster-of-cluster aggregates. Specifically, trivalent lanthanide cations have been used as linkages owing to their high coordination number and flexible coordination environment, which place few structural restrictions on the resulting architectures. The principle can be best exemplified by a pioneering study by Pope et al., who reported the self-assembly of a giant water soluble tungstate, $[As_{12}Ce_{16}(H_2O)_{36}W_{148}O_{524}]^{76-}$.[9] In the structure, the Ce^{III} cations bridge twelve trilacunary $[AsW_9O_{33}]^{9-}$ and four mono-lacunary $[W_5O_{18}]^{6-}$ units. The spherical superstructure is ca. 4 nm in diameter and is water-soluble, highlighting that this compound class is at the borderline between molecular and nanoparticulate metal oxides. The assembly of the compound proceeds under one-pot conditions by reaction of simple oxometalate precursors in aqueous phase, highlighting that metal-oxide self-assembly strategies can generate highly complex nanostructures.

Building on these seminal studies, even more complex architectures have been assembled, see Table S1 in the Supporting Information for a summary. In 2007, Kortz et al. reported the cerium germanotungstate $[Ce_{20}Ge_{10}W_{100}O_{376}(OH)_4(H_2O)_{30}]^{56-}$, which features 130 metal ions and can be considered as a dimeric structure based on two identical subunits.[10] In 2009, Patzke et al. reported a giant gadolinium-linked tungstate cluster, $[Gd_8As_{12}W_{124}O_{432}(H_2O)_{22}]^{60-}$, featuring 154 metal ions and a length of almost 5 nm.[11] In 2012, Cronin et al. used a networked reactor system under flow to synthesize the giant cobalt tungstate $[H_{16}Co_8W_{200}O_{660}(H_2O)_{40}]^{88-}$.[12] Recently, Zhao et al. reported one of the first application-driven studies in the field and showed that lanthanide tungstate aggregates $\{[Ln_{10}W_{16}(H_2O)_{30}O_{50}](B\text{-}\alpha\text{-}AsW_9O_{33})_8\}^{46-}$ (Ln = trivalent lanthanide) exhibit anticancer properties against several cancerous cell lines.[13] Intriguingly, most syntheses of giant tungstates rely on trilacunary Keggin fragments (e.g. $[B\text{-}\alpha\text{-}XW_9O_{33}]^{n-}$, X = ($As^{III}$, Sb^{III}, Bi^{III}, Se^{IV}, Te^{IV}, etc.) featuring a central template with trigonal pyramidal geometry, XO_3^{n-}. Based on structural considerations and previous studies, it can be suggested that the lone electron pair on this template prevents the direct coordination of metal ions, so that the formation of small clusters is prevented.[9,10,13–15]

We rationalized that other trivalent metal cations, such as bismuth(III), could be used together with lanthanide cations for the linkage and stabilization of giant tungstate clusters. This is based on the idea that the large size of Bi^{III} makes it ideal for linking POMs. When incorporated into tungstate clusters, Bi^{III} ions enable the formation of lacunary clusters by preventing full closure of the tungstate shell due to the presence of a lone electron-pair on Bi^{III}. Further, Nyman et al.[16] and Streb et al.[17] recently demonstrated that Bi^{III} ions are well suited for stabilizing labile POM aggregates. In addition, using lanthanide cations such as $Ce^{III/IV}$ can harness their high coordination number and oxophilicity to link neighboring tungstate clusters. Notably, the development of bismuth-functionalized POMs is still a major challenge, as reaction of bismuth precursors with tungstates and/or lanthanides typically leads to insoluble precipitates.

Herein, we explored the bismuth-cerium-tungstate reaction system and report the self-assembly of a giant POM aggregate by one-pot reaction of $Na_2WO_4{\cdot}2H_2O$, $NaAc{\cdot}3H_2O$, $Bi(NO_3)_3{\cdot}5H_2O$, and $(NH_4)_2Ce(NO_3)_6$ in acidic aqueous medium. Upon crystallization, the reaction gave yellow needle crystals suitable for single-crystal X-ray diffraction (Figure S1 in the Supporting Information). The compound crystallized in the monoclinic space group $C2/c$ with cell parameters of $a = 34.540(5)$ Å, $b = 31.408(4)$ Å, $c = 41.760(6)$ Å, $\beta = 109.152(2)°$, $V = 42796$ Å^3, for details see Table S2. Structure analysis showed a bismuth

[*] J.-C. Liu, Q. Han, Dr. L.-J. Chen, Prof. Dr. J.-W. Zhao
Henan Key Laboratory of Polyoxometalate Chemistry, Institute of Molecular and Crystal Engineering, College of Chemistry and Chemical Engineering, Henan University
Kaifeng, Henan 475004 (China)
E-mail: zhaojunwei@henu.edu.cn
zhaojunwei@vip.henu.edu.cn
J.-C. Liu, Prof. Dr. Y.-F. Song
State Key Laboratory of Chemical Resource Engineering
Beijing University of Chemical Technology
Beijing 100029 (China)
E-mail: songyufei@hotmail.com
songyf@mail.buct.edu.cn
Prof. Dr. C. Streb
Institute of Inorganic Chemistry I
Ulm University
Albert-Einstein-Allee 11, 89081 Ulm (Germany)
E-mail: carsten.streb@uni-ulm.de
Supporting information and the ORCID identification number(s) for the author(s) of this article can be found under: https://doi.org/10.1002/anie.201803649.

cerium tungstate cluster with the sum formula $Na_{16}(NH_4)_{10}H_8\{[W_{14}Ce^{IV}{}_6O_{61}](W_3Bi_6Ce^{III}{}_3(H_2O)_3O_{14}]$-$[\alpha\text{-}BiW_9O_{33}]_3)_2\}\cdot$ca. $38\,H_2O$ ($=Na_{16}(NH_4)_{10}H_8$**1** ca. $38\,H_2O$). Compound **1** features dimensions of ca. $3.0\times2.0\times1.7$ nm^3 and has C_{2v} symmetry, see Figure 1 and Figure 2. The structure, elemental composition and phase purity of **1** were confirmed by single-crystal XRD, elemental analysis, X-ray photoelectron spectroscopy (XPS), powder-X-ray diffraction, thermogravimetry and FT-IR spectroscopy (Figure S3–S5).

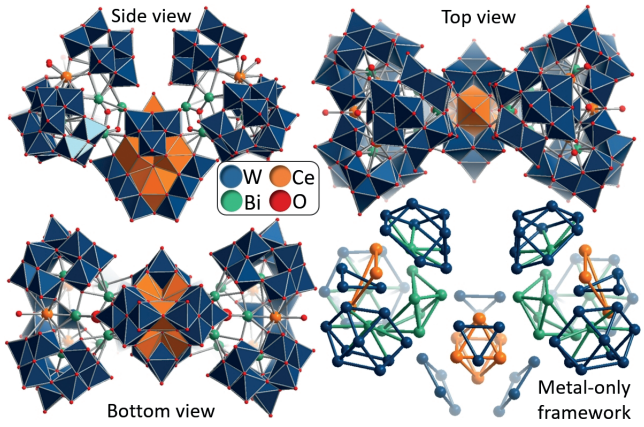

Figure 1. Polyhedral representation of the supramolecular cluster anion **1** as identified by single-crystal X-ray diffraction. The metal-only framework shows the positions of the Bi, Ce, and W metal ions. Note that the "bonds" drawn between individual metals in the "metal-only framework" illustration do not represent covalent interactions but are used to emphasize secondary building units. For CCDC number see Supporting Information.

Compound **1** represents an unprecedented bismuth-cerium tungstate cluster-of-clusters anion which can be separated into several secondary building units (SBUs). Structural features of **1** are discussed based on the metal center positions only for reasons of clarity. The center of the cluster anion is formed by an octahedral arrangement of six cerium centers, giving the **{Ce$_6$}** building unit (diameter ca. 0.5 nm, Figure 2). Bond valence sum calculations (BVS) based on single-crystal XRD data show that the Ce ions are in oxidation state +IV. Opposite faces of the **{Ce$_6$}** octahedron are capped by two **{W$_3$}** and two **{W$_4$}** SBUs. The **{W$_3$}** unit is based on a triangular arrangement of three edge-sharing [WO_6] octahedra and can be considered as one half of the Lindqvist anion $[M_6O_{19}]^{2-}$.[18] Alternatively, **{W$_3$}** can be described as one of the so-called "triads" forming SBUs of the famous Keggin anion.[17] The **{W$_4$}** unit is based on four edge-sharing [WO_6] octahedra and is isostructural to one half of the β-octamolybdate anion $[\beta\text{-}Mo_8O_{26}]^{4-}$.[19,20] BVS calculations confirm that all W centers are in oxidation state +6. Further, two faces of the central **{Ce$_6$}** octahedron are capped by **{Bi$_6$}** units. **{Bi$_6$}** is capped by three trilacunary **{BiW$_9$}** ($=[B\text{-}\alpha\text{-}BiW_9O_{33}]^{9-}$) units arranged in an isosceles triangle. Finally, this arrangement is capped by a **{Ce$_3$W$_3$}** unit, where BVS calculations indicate the presence of Ce^{3+} and W^{6+}.

In the crystal lattice, **1** forms a 3D framework, where individual anions are linked electrostatically by Na^+ and NH_4^+ cations. The lattice shows a complex 3D pore architecture (Figure 3) featuring water-filled channels with maximum pore diameters of approx. 0.5–0.6 nm (Figure 3). Crystallographic analysis of the pore structure (probe radius 1.2 Å) indicates a solvent-accessible volume of approximately 20% (ca. 8500 Å^3).

We hypothesized that the resulting intra-channel hydrogen bonding network between water molecules and ammonium cations could enable proton transport, either via a Grotthuss (proton hopping) or a vehicle (diffusion of charged proton carries, for example, H_3O^+) mechanism.[21] Porous framework materials, for example, metal–organic frameworks (MOFs), have recently gained significant interest for proton conduction due to their modular assembly high stability and chemical tunability.[22–24] In contrast, POM-based frameworks[2,25] for proton conduction are still in their infancy, and have only recently received significant attention,[22,23,26–28] although proton conduction in solid POMs has

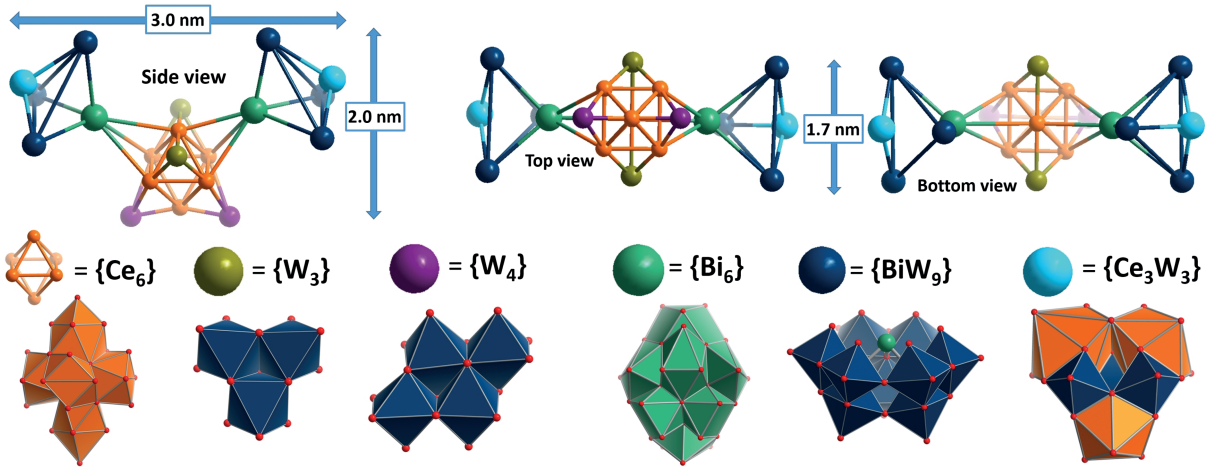

Figure 2. Rationalization of the structural features of **1**, highlighting the central **{Ce$_6$}** core which is capped by two **{W$_3$}** and two **{W$_4$}** units. Large peripheral groups consisting of a **{Bi$_6$}** unit capped by three **{BiW$_9$}** lacunary Keggin ions and a **{Ce$_3$W$_3$}** moiety further stabilize the central unit.

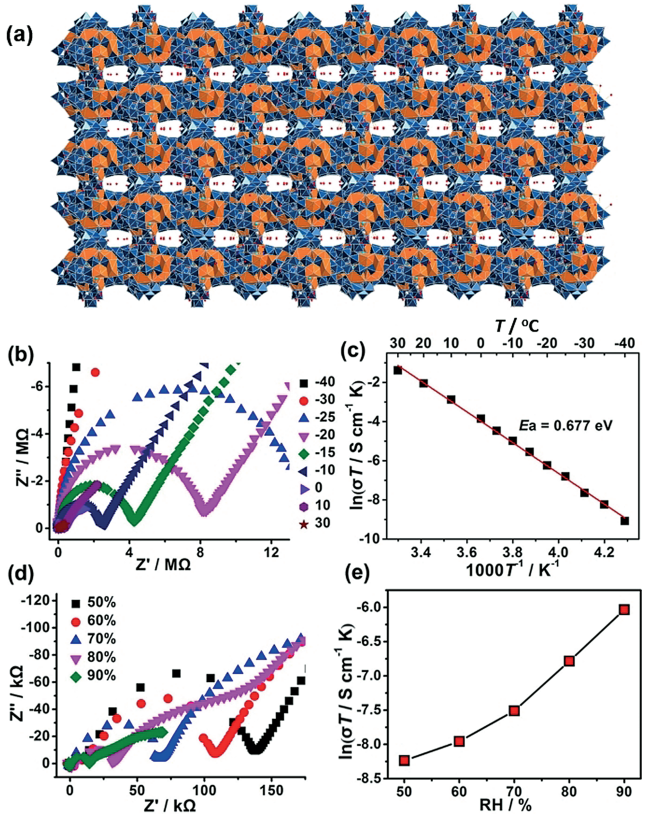

Figure 3. a) Illustration of the porous framework of **1** (19.6 vol% solvent accessible voids). b) Nyquist plots for **1** under anhydrous conditions at $T = -40$–$30\,^{\circ}C$. c) Arrhenius plot for **1** under anhydrous conditions. Least-square fitting shown as a solid line; d) Nyquist plot for **1** under relative humidity between 50% to 90% RH at $T = 25\,^{\circ}C$; e) Proton conductivity of **1** as a function of RH (25 °C).

been known since the initial report by Nakamura et al. in 1979.[29] Thus, we decided to study the proton conductivity of **1** using alternating current electrochemical impedance spectroscopy (AC-EIS) of dry, powdered samples of **1** under anhydrous conditions at AC frequencies between 10^7 and 1 Hz. Data analysis was performed based on Nyquist plots (Figure 3 and Supporting Information). Proton conductivity in solids is highly dependent on temperature and relative humidity (RH) of the environment.[21] We therefore explored the effects of these parameters on the proton conductivity of **1**. We also explored proton conductivity below the freezing point of water (down to −40 °C), as mechanical damage to the sample based on solidification (freezing) of water can be a significant impediment.

We observed structural integrity and retention of proton conductivity across the temperature range studied: at −40 °C a proton conductivity of $4.9 \times 10^{-7}\,S\,cm^{-1}$ is observed. To our knowledge, this is the first report of POM-based anhydrous proton conductivity below 0 °C. Notably, the reported values are some of the highest conductivities reported at sub-zero temperatures to-date and can be compared with leading porous materials such as mesoporous organic imide frameworks (proton conductivity up to $2.2 \times 10^{-6}\,S\,cm^{-1}$.[30] With increasing temperature, the proton conductivity of **1** rapidly increases by three orders of magnitude to $8.3 \times 10^{-4}\,S\,cm^{-1}$ at 30 °C (Figure 3 and Supporting Information), indicating that elevated temperatures promote the proton transport.

The activation energy (E_a) of **1** derived from the Arrhenius equation ($\sigma_T = \sigma_0 \exp(-E_a/k_B T)$) was calculated to 0.677 eV (Figure 3), indicating a vehicle mechanism,[21,28] where proton transport is due to the diffusion of charged "proton-carrier" molecules, for example, H_3O^+ or NH_4^+.[24] This is the most common mechanism of proton transport in aqueous systems.

The proton conductivity of **1** was also measured at relative humidities (RH) between RH = 50% to 90% at $T = 25\,^{\circ}C$, see Figure 3. Increasing humidity results in increasing proton conductivity between $2.6 \times 10^{-4}\,S\,cm^{-1}$ (50% RH) and $2.4 \times 10^{-3}\,S\,cm^{-1}$ (90% RH). This indicates that water adsorption can be used to tune proton conductivity, suggesting that in principle, atmospheric water sensing by **1** is possible. In addition, we note that **1** features one of the highest proton conductivities for POM-based materials at low RH (50%, see Table S4 for comparative data).

In summary, we report the assembly of the first giant cerium–bismuth tungstate cluster by a simple self-assembly procedure under one-pot conditions. The compound is fully structurally characterized and its assembly from virtual secondary building units and several prominent POM cluster fragments is rationalized. The compound shows unique structural features in the crystalline state and combines 3D porosity with high proton conductivity. The materials design approach could in future be used to access advanced metal oxide framework components for proton conductivity applications under harsh environmental conditions as required for example, for fuel cells.

Acknowledgements

Dr. G. Xu (Fujian Institute of Research on the Structure of Matter,Chinese Academy of Sciences) is acknowledged for support in proton conductivity analysis. This work was supported by the Natural Science Foundation of China, the National Basic Research Program of China (973 program, 2014CB932104), the Innovation Scientists and Technicians Troop Construction Projects of Henan Province (174100510016) and the Program for Science & Technology Innovation Talents in Universities of Henan Province (16HASTIT001) and Deutsche Forschungsgemeinschaft DFG (INST 40/505-1 FUGG).

Conflict of interest

The authors declare no conflict of interest.

Keywords: polyoxometalates · polyoxotungstate · porous materials · proton conduction · self-assembly

How to cite: *Angew. Chem. Int. Ed.* **2018**, *57*, 8416–8420
Angew. Chem. **2018**, *130*, 8552–8556

[1] D. L. Long, R. Tsunashima, L. Cronin, *Angew. Chem. Int. Ed.* **2010**, *49*, 1736 – 1758; *Angew. Chem.* **2010**, *122*, 1780 – 1803.
[2] L. Vilà-Nadal, L. Cronin, *Nat. Rev. Mater.* **2017**, *2*, 17054.
[3] D.-L. L. Long, E. Burkholder, L. Cronin, *Chem. Soc. Rev.* **2007**, *36*, 105 – 121.
[4] (Guest Eds.: L. Cronin, A. Müller), *Chem. Soc. Rev.* **2012**, *41*, 7325 – 7648.
[5] (Guest Ed.: C. L. Hill), *Chem. Rev.* **1998**, *98*, 1 – 301.
[6] (Guest Eds.: U. Kortz, T. Liu), *Eur. J. Inorg. Chem.* **2013**, 1556 – 1967.
[7] L. Cronin, *Comprehensive Coordination Chemistry II*, *Vol. 7*, Elsevier, Amsterdam, **2004**, pp. 1 – 56.
[8] M. T. Pope, Y. Jeannin, M. Fournier, *Heteropoly and Isopoly Oxometalates*, Springer, Heidelberg, **1983**.
[9] K. Wassermann, M. H. Dickman, M. T. Pope, *Angew. Chem. Int. Ed. Engl.* **1997**, *36*, 1445 – 1448; *Angew. Chem.* **1997**, *109*, 1513 – 1516.
[10] B. S. Bassil, M. H. Dickman, I. Römer, B. Von Der Kammer, U. Kortz, *Angew. Chem. Int. Ed.* **2007**, *46*, 6192 – 6195; *Angew. Chem.* **2007**, *119*, 6305 – 6308.
[11] F. Hussain, F. Conrad, G. Patzke, *Angew. Chem. Int. Ed.* **2009**, *48*, 9088 – 9091; *Angew. Chem.* **2009**, *121*, 9252 – 9255.
[12] A. R. de la Oliva, V. Sans, H. N. Miras, J. Yan, H. Zang, C. J. Richmond, D. L. Long, L. Cronin, *Angew. Chem. Int. Ed.* **2012**, *51*, 12759 – 12762; *Angew. Chem.* **2012**, *124*, 12931 – 12934.
[13] J.-W. Zhao, H.-L. Li, X. Ma, Z. Xie, L.-J. Chen, Y. Zhu, *Sci. Rep.* **2016**, *6*, 26406.
[14] K. Fukaya, T. Yamase, *Angew. Chem. Int. Ed.* **2003**, *42*, 654 – 658; *Angew. Chem.* **2003**, *115*, 678 – 682.
[15] S. Reinoso, M. Giménez-Marqués, J. R. Galán-Mascarós, P. Vitoria, J. M. Gutiérrez-Zorrilla, *Angew. Chem. Int. Ed.* **2010**, *49*, 8384 – 8388; *Angew. Chem.* **2010**, *122*, 8562 – 8566.
[16] a) P. I. Molina, K. Kozma, M. Santala, C. Falaise, M. Nyman, *Angew. Chem. Int. Ed.* **2017**, *56*, 16277 – 16281; *Angew. Chem.* **2017**, *129*, 16495 – 16499; b) O. Sadeghi, M. Amiri, E. Reinheimer, M. Nyman, *Angew. Chem. Int. Ed.* **2018**, https://doi.org/10.1002/anie.201802915; *Angew. Chem.* **2018**, https://doi.org/10.1002/ange.201802915.
[17] J. Tucher, L. C. Nye, I. Ivanovic-Burmazovic, A. Notarnicola, C. Streb, *Chem. Eur. J.* **2012**, *18*, 10949 – 10953.
[18] S. Herrmann, J. T. T. Margraf, T. Clark, C. Streb, *Chem. Commun.* **2015**, *51*, 13702 – 13705.
[19] M. T. Pope, A. Müller, *Angew. Chem. Int. Ed. Engl.* **1991**, *30*, 34 – 48; *Angew. Chem.* **1991**, *103*, 56 – 70.
[20] E. F. Wilson, H. Abbas, B. J. Duncombe, C. Streb, D.-L. Long, L. Cronin, *J. Am. Chem. Soc.* **2008**, *130*, 13876 – 13884.
[21] K.-D. Kreuer, *Chem. Mater.* **1996**, *8*, 610 – 641.
[22] M. Yoon, K. Suh, S. Natarajan, K. Kim, *Angew. Chem. Int. Ed.* **2013**, *52*, 2688 – 2700; *Angew. Chem.* **2013**, *125*, 2752 – 2764.
[23] S. Uchida, R. Hosono, R. Eguchi, R. Kawahara, R. Osuga, J. N. Kondo, M. Hibino, N. Mizuno, *Phys. Chem. Chem. Phys.* **2017**, *19*, 29077 – 29083.
[24] G. K. H. Shimizu, J. M. Taylor, S. Kim, *Science* **2013**, *341*, 354 – 355.
[25] H. N. Miras, L. Vilà-Nadal, L. Cronin, *Chem. Soc. Rev.* **2014**, *43*, 5679 – 5699.
[26] a) H. Ma, B. Liu, B. Li, L. Zhang, Y.-G. Li, H.-Q. Tan, H.-Y. Zang, G. Zhu, *J. Am. Chem. Soc.* **2016**, *138*, 5897 – 5903; b) Y.-Q. Jiao, H.-Y. Zang, X.-L. Wang, E.-L. Zhou, B.-Q. Song, C.-G. Wang, K.-Z. Shao, Z.-M. Su, *Chem. Commun.* **2015**, *51*, 11313 – 11316.
[27] Z. Li, X.-X. Li, T. Yang, Z.-W. Cai, S.-T. Zheng, *Angew. Chem. Int. Ed.* **2017**, *56*, 2664—2669; *Angew. Chem.* **2017**, *129*, 2708—2713.
[28] A. Shigematsu, T. Yamada, H. Kitagawa, *J. Am. Chem. Soc.* **2011**, *133*, 2034 – 2036.
[29] O. Nakamura, T. Kodama, I. Ogino, Y. Miyake, *Chem. Lett.* **1979**, *8*, 17 – 18.
[30] Y. Ye, L. Zhang, Q. Peng, G.-E. Wang, Y. Shen, Z. Li, L. Wang, X. Ma, Q.-H. Chen, Z. Zhang, S. Xiang, *J. Am. Chem. Soc.* **2015**, *137*, 913 – 918.

Manuscript received: March 26, 2018
Accepted manuscript online: April 23, 2018
Version of record online: May 14, 2018

